

TOMASZ GĘBAROWSKI*, MARCIN JARACZEWSKI**, RYSZARD MIELNIK***

THE LOW-FREQUENCY MEASURING METHOD OF VOLTAGE, CURRENT, POWER AND SIGNAL PROCESSING APPLICATION FOR COMPACT PLC

APLIKACJA NISKOCZĘSTOTLIWOŚCIOWEJ METODY POMIARU NAPIĘCIA, PRĄDU I MOCY NA KOMPAKTOWYM STEROWNIKU PLC

Abstract

This article presents the implementation of the low-frequency measuring method of current and voltage RMS values as well as active and reactive power of a two-terminal network, which is supplied by a sinusoidal voltage of 50 Hz. The implementation was made on a typical compact PLC-FX3G Mitsubishi Electric controller. This controller has a relatively low computing power, and when control tasks and measurements are performed simultaneously, the measurement method must be simple in order to match the limited computing power of the controller. This article describes how to implement the low-frequency measuring method onto the controller. It also presents the laboratory set for testing the controller and application. The paper also presents the results of measurements and calculations, in particular the impact of measurement time delays on errors of the RMS voltage and current values as well as active and reactive power values.

Keywords: digital measurement of voltage, current and power, PLCs, measuring errors

Streszczenie

W artykule przedstawiono implementację niskoczęstotliwościowej metody pomiaru wartości skutecznej prądu i napięcia oraz mocy czynnej P i biernej Q na dwójniku zasilanym napięciem sinusoidalnym 50 Hz. Aplikacja została wykonana na typowym, kompaktowym sterowniku PLC typu FX3G firmy Mitsubishi. Sterownik ten posiada stosunkowo małą moc obliczeniową i dlatego też w przypadku wykonywania zadań sterowniczych i pomiaru parametrów sygnałów, musi mieć zaimplementowaną prostą, nie wymagającą nadmiernej mocy obliczeniowej metodę pomiaru parametrów sygnału. W artykule przedstawiono sposób implementacji niskoczęstotliwościowej metody pomiaru prądu, napięcia i mocy. Przedstawiono stanowisko laboratoryjne do testowania wykonanej aplikacji na sterowniku PLC. Uzyskane wyniki poddano analizie i przedstawiono wyniki badań, a w szczególności przedstawiono wpływ opóźnień czasowych na błędy uzyskanych wyników pomiarowych.

Słowa kluczowe: cyfrowy pomiar napięcia, prądu i mocy, sterowniki PLC, błędy pomiarowe

* Eng. Tomasz Gębarowski, Mitsubishi Electric Europe B.V., branch in Poland, Cracow.

** Ph.D. Eng. Marcin Jaraczewski, Institute of Industrial Electrical Engineering and Technical Computer Science, Faculty of Electrical and Computer Engineering, Cracow University of Technology.

*** Ph.D. Eng. Ryszard Mielnik, Institute of Electromechanical Energy Conversion, Faculty of Electrical and Computer Engineering, Cracow University of Technology.

1. Introduction

For the time being, the techniques used for power and RMS value measurements are carried out by digital data acquisition boards that use a high sampling frequency and require a large number of samples per period of measured signal [6]. These techniques obeyed the Nyquist (Shannon) law, which requires at least two samples of measured signal per period. For example, according to this criterion, at least an $f_s = 100$ Hz sampling rate is needed to measure a 50 Hz sinusoidal signal. In practice, this sampling frequency reaches up to a few kHz. Similarly, the widely used integral formulas for the determination of power and RMS values of input signals are computationally expensive, i.e. require expensive digital processing systems and processors.

This article presents a different approach to the measurement and calculation of the active and reactive power as well as the RMS voltage and current values of load, supplied by a 50 Hz sinusoidal voltage. This method uses a low sampling frequency f_s , such as 8 Hz [2, 3]. When such a low sampling frequency is applied ($f_s < 50$ Hz) in the measurement, the use of sophisticated measuring systems and expensive processors is no longer needed, but only simple and inexpensive ones [5]. The article presents the application of this method on a compact PLC FX3G type made by Mitsubishi Electric, classified as a lower level performance controller. From the economic point of view, this controller is also one of the cheapest PLC. The article presents the laboratory set and the application used to measure and process the sampled voltage and current in order to calculate their RMS values as well as active and reactive power values. It also presents the error analysis of the measured voltage, current and power, which result from the impact of PLC time delays on the calculations.

2. Low frequency measurement method for power and RMS value evaluation

This measuring method, used to determine active and reactive input power of the two-terminal network, and its RMS voltage and current values, can be applied only for an AC alternating sinusoidal voltage and current. The method consists in [2] measuring the instantaneous values of the voltage and current of the two-terminal network, first at time t_1 and after at t_2 . Thus, the two pairs of values $u_1 = u(t_1)$, $i_1 = i(t_1)$ for the first measurement and $u_2 = u(t_2)$, $i_2 = i(t_2)$ are obtained for the second measurement. Then, according to the formulas presented in [2, 3], the active P and reactive Q power as well as the RMS values of sinusoidal current and voltage can be calculated as:

$$P = \frac{i_1 u_1 + i_2 u_2}{2}, \quad Q = \frac{(u_1 i_2 - u_2 i_1)}{2} \quad (1)$$

$$I_{\text{RMS}} = \sqrt{\frac{i_1^2 + i_2^2}{2}}, \quad U_{\text{RMS}} = \sqrt{\frac{u_1^2 + u_2^2}{2}} \quad (2)$$

where:

$u_1 = u(t_1)$; $u_2 = u(t_2)$ – two consecutive samples of voltage signal taken at the time t_1 and t_2 ,

$i_1 = i(t_1)$; $i_2 = i(t_2)$ – two consecutive samples of current signal taken at the time t_1 and t_2 .

The scheme of samples taking voltage and current sinusoidal signals is shown in Fig. 1a [2].

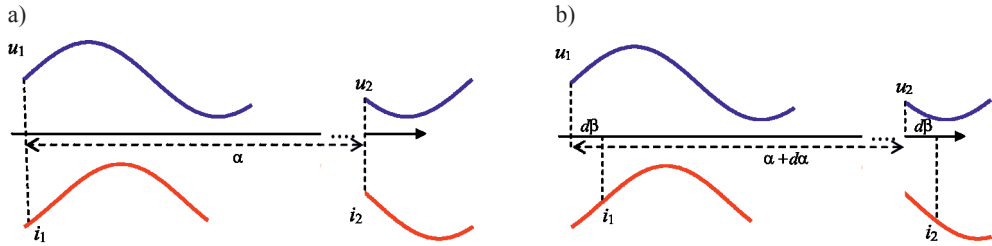


Fig. 1. a) theoretical (parallel) sampling of voltage and current, b) real (serial) sampling of voltage and current

The sampling frequency f_s , which determines the phase interval between the two consecutive samples of voltage $u_1(t_1)$, $u_2(t_2)$ and current $i_1(t_1)$, $i_2(t_2)$, can be calculated from equation:

$$\alpha = \omega(t_2 - t_1) = \omega T_s = \frac{2\pi f}{f_s} = (2n+1) \frac{\pi}{2} \quad (3)$$

where:

- $T_s = 1/f_s$ – sampling period,
- f_s – sampling rate,
- f – signals frequency,
- n – positive integer.

When the two-terminal network is supplied by a sinusoidal signal of $f = 50$ Hz, the sampling rate f_s is given by:

$$f_s = 4 \frac{f}{2n+1} = 200 \frac{1}{2n+1} \quad (4)$$

and the sampling period is:

$$T_s = n \cdot 10 + 5 \text{ [ms]} \quad (5)$$

Fig. 2 shows the algorithm used for the measurement and calculation of the current and voltage RMS values and the active/reactive power of a two-terminal network [2]. At first, the time interval T_s is set; then, if the time required for this interval elapses; a pair of instantaneous current I_1 and voltage U_1 is readout.

Next, these values are scaled. In the following steps, the RMS values of current I_{RMS} , voltage U_{RMS} and active P , reactive Q power are calculated. The last step of the algorithm records the current value of I_1 and U_1 as I_2 and U_2 variables that are required in the next iteration of the algorithm. After storing the measured values of voltage and current, the condition to start the next iteration of the algorithm is checked. This condition is an information whether the next interval T_s elapsed. If this interval elapsed, the next iteration of the algorithm starts, which measures new values of the instantaneous current I_1 and

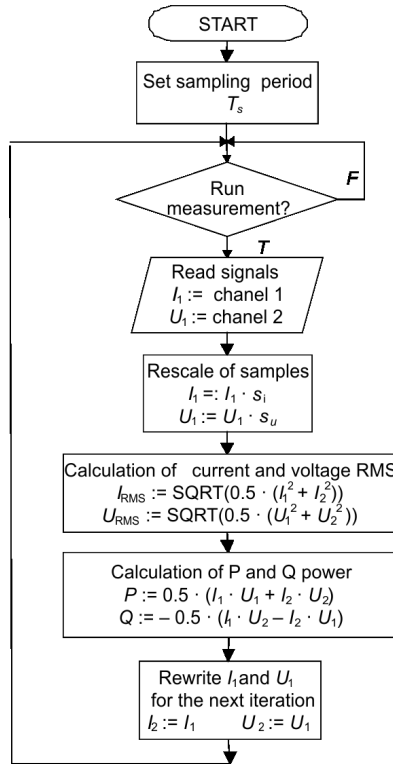


Fig. 2. The algorithm for measurement and calculation of the current and voltage RMS values and active P and reactive Q power, for given T_s time interval

voltage U_1 . At the same time, the algorithm uses the previously stored instantaneous values of current I_2 and voltage U_2 . Therefore, the correct results of current I_{RMS} and voltage U_{RMS} RMS values and active P and reactive Q power are obtained after two algorithm iterations.

If the sampling of voltage and current is carried out by real analogue – digital A/C converter, this sampling process is not really parallel, but rather series, as it is shown in Fig.1b. The resulting time delay between the voltage and current sample readout time, as well as T_s time inaccuracy, introduces a calculation error of active P and reactive Q power.

Relative error [1] of active power P can be calculated by the following formula:

$$\frac{P - P_0}{P_0} = dP + d\tilde{P} \quad (6)$$

where:

- P, P_0 – measured and accurate value of active power
- average relative error is:

$$dP = \frac{1}{\cos(\phi)} (\cos(\phi - d\beta) - \cos(\phi))$$

when assuming $d\beta$ is small, thus:

$$dP \approx \operatorname{tg}(\phi)d\beta \quad (7)$$

– oscillating relative error is:

$$d\tilde{P} = \frac{1}{2 \cos(\phi)} (\cos(2\omega t_1 - \phi + d\beta) - \cos(2\omega t_1 - \phi + d\beta + 2d\alpha))$$

when assuming $d\alpha$ is small, thus:

$$d\tilde{P} = \frac{\sin(\phi - d\beta - 2\omega t_1)}{2 \cos(\phi)} d\alpha \quad (8)$$

ϕ – phase angle of the receiver,

ωt_1 – phase angle of the first voltage sample,

$d\alpha$ – inaccuracy of period (T_s),

$d\beta$ – delay time between consecutive voltage-current samples.

And relative error [1] of Q measurement is given by:

$$\frac{Q - Q_0}{Q_0} = \frac{1}{2 \sin(\phi)} (\sin(\phi - d\alpha + d\beta) + \sin(\phi - d\alpha - d\beta)) - 1$$

when assuming $d\alpha$ is small, thus:

$$\frac{Q - Q_0}{Q_0} \approx \operatorname{cotg}(\phi)d\alpha \quad (11)$$

where:

Q, Q_0 – measured and accurate value of reactive power.

3. Implementation of the low-frequency method on PLC

A wide range of small PLC is used typically for not very demanding applications, i.e. control tasks that do not require a big computing power. Effective implementation of the low-frequency measuring method, for this type of PLCs, must ensure not only a proper and uninterrupted control operation, but also monitoring the active, reactive supply power and the voltage, current RMS values.

3.1. Compact FX3G type PLC

FX3G is one of the programmable devices of MELSEC-F (Mitsubishi Electric Sequence Control) series and it is the third generation of compact, standard controllers of FX3 series [10]. The FX3G controller in its single chassis integrates the power supply, CPU, I/O points and the communication interface. Using a wide range of expansion boards, the functionality of the PLC can be extended to an application requirement.

Normally, to carry out the 50 Hz voltage and current sampling process, the FX3G-2AD-BD expansion boards for two analogue inputs (hereinafter called 2AD-BD) is used [7, 11], which is mounted to the controller in a special slot. The signals from two analogue channels of that board are converted into digital samples using the serial analogue to digital method of conversion.

Configuration of the A/C board is done by the user application, by setting the special register's bits dedicated for this purpose [8, 11]. You can also choose the type of the input analogue signal (voltage or current) and the amount of collected samples (in the range of 1 to 4095). In each cycle of the controller, if necessary, register and bit settings of the A/C board can be modified in the application. Also, in each controller cycle, the digital samples, after the A/C conversion, are stored in a special memory area as the global variables. During the controller's operating cycle, the status of the A/C board is also readout. In the case of errors, an error code is generated. The simple diagnostics of the A/C board recognise the input signal over-range, averaging error, hardware and communication error.

3.2. Implementation of the measuring algorithm on PLC

Application of the low-frequency measuring method of voltage, current and power requires a specified readout time interval T_s . This time interval must be measured off with high accuracy and stability over time. Therefore, in order to achieve this, one of three interval interrupts from the FX3G (Tab. 1) controller has been used, which range between 0 and 99 ms every 1 ms [10]. For proper and efficient operation of the controller application, it was divided into subroutines [13, 14]. These subroutines must implement the readout of voltage and current samples, calculation of the RMS values of voltage and current, the active and reactive power calculation and the control tasks. A complete controller cycle is shown in Fig. 3.

After starting, the PLC reads out the state of inputs and creates an image of their values in the memory area. Next, the following subroutines are executed:

- **subroutine_0** (executed only once, at start-up) – configures the A/C board, transmission interface and variables defined in the user application,
- **subroutine_1** – implements the functions of the control tasks,
- **subroutine_2** – calculates the voltage and current RMS values as well as the active and reactive power with the use of previous and current measured values stored as global variables,
- **Subroutine_3** –sends the currently measured and calculated values using the so-called no-protocol data transmission protocol [9, 13].

Subroutine_1, **subroutine_2** and **subroutine_3** are executed sequentially, in each cycle of the PLC.

Subroutine_INT is called the 'time interruption subroutine', because in the PLC run mode [12, 13] (this mode is marked as a dashed line, see Fig. 3), it is called exactly when the interrupt occurs. This interval of interruptions is set in **subroutine_0** as a variable T_s . **Subroutine_INT** moves the measurement samples from two registers dedicated to the A/C board (channel 1 and 2) to the global variables, used after in **subroutine_2**. After this,

subroutine_INT returns to the controller’s operating cycle at exactly the same point where it was called from. However, if the interruption occurs outside the program (at the scan time), the channels are read out as soon as PLC enters program execution mode [13, 14]. In order to eliminate the time shift, a constant run-time of the PLC cycle is imposed – Fig. 4.

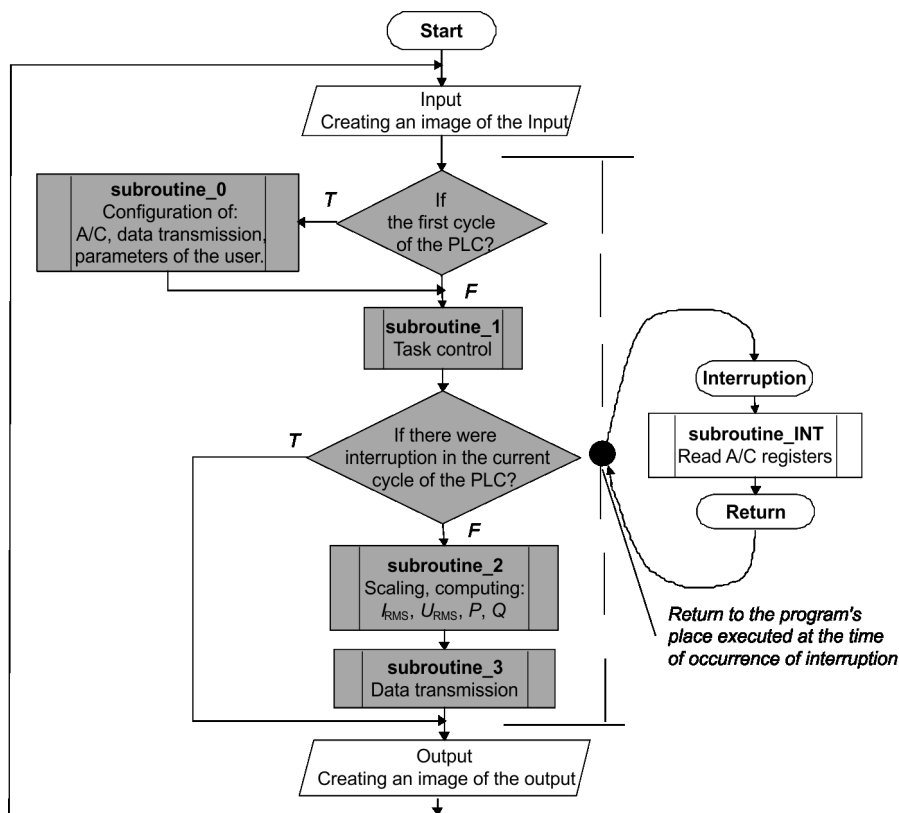


Fig. 3. PLC cycle with measurement and control tasks

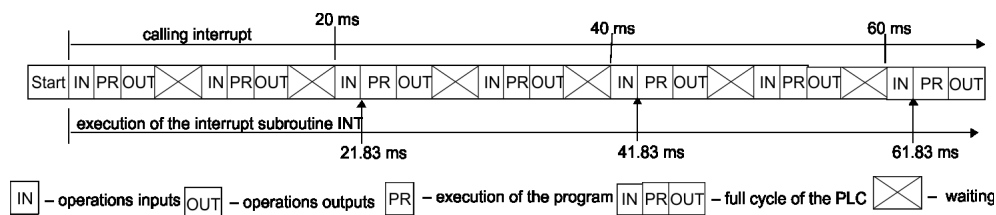


Fig. 4. A constant cycle-time of PLC

This cycle-time must be a T_s integer divider. This way, regardless of the call moment of the subroutine_INT, the time interval will always be the same, providing a constant time interval T_s . The cycle-time of controller must ensure complete execution of whole algorithm. This time can

be read out from a special controller's register storing the maximum cycle's time [13, 14]. The cycle-time must be longer than the maximum execution, 15 time of the application. The time needed for measurement, calculations and control task was about 1.6 ms, whereas the constant cycle time of the controller was set to 5 ms. Such controller's cycle time value allows to carry out measurements for different T_s intervals because their values are always integer multiples of 5 ms.

4. Laboratory station for application testing

In order to verify the implemented algorithm on PLC, a test stand was built and a simulated virtual RLC load has been used. Fig. 5 shows a block diagram of the laboratory station for PLC application testing.

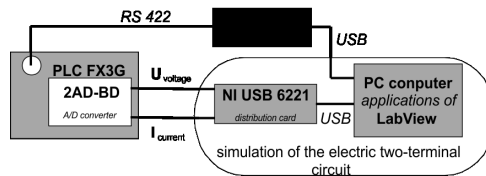


Fig. 5. The block diagram of the laboratory station to test the PLC application

The laboratory station consist of:

- the FX3G-24MT/DSS controller (12 inputs and 12 digital outputs), two-channel A/C expansion board FX3G-2AD-BD, the communication interface RS-422,
- the universal input/output card made by National Instruments NI USB 6221 type with 2 analogue output channels ± 10 V,
- a PC computer with the installed LabVIEW environments.

The first LabVIEW application allows to set the desired values of active and reactive power of a two-terminal network, then two analogue outputs of the USB NI 6221 card generate the current and voltage of 50 Hz sinusoidal signals, meeting the desired P , Q values of virtual electric load. The generated analogue signals are in the range of 0–10 V, in order to meet the measuring range of analogue channels of A/C expansion board 2AD-BD of FX3G controller. The second application, created with LabVIEW, reads out, via the serial RS 422 interface, the measured and calculated RMS voltage, current and power values from the FX3G controller [9]. These values are then saved in data files for further use in analysis.

The laboratory station, of which block diagram is in Fig. 5, has been used to check the time interval between consecutive samples of current and voltage read out by PLC.

5. The results of measurements and errors estimation

The sample's reading delay of an analog-digital 2AD-BD expansion board, both in the voltage and the current channel, has been measured with the use of the LabVIEW generator, using a reference sawtooth voltage with a changeable α period, which corresponded to different T_s periods.

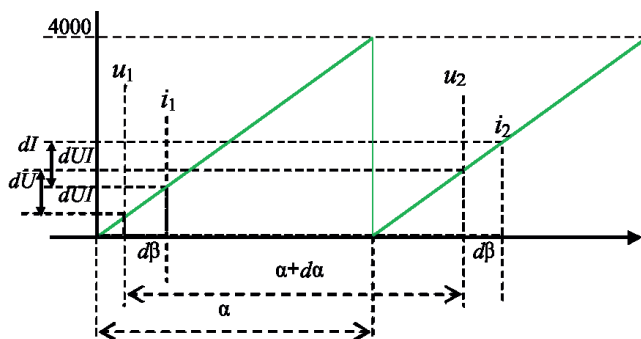


Fig. 6. Sample's readout time in voltage and current channels measured using the reference sawtooth voltage signal

According to Fig. 8 and after a conversion to appropriate degrees, corresponding to the 50 Hz signal, the following formulas are obtained:

$$d\alpha U = \alpha \frac{dU}{4000}, \quad d\alpha I = \alpha \frac{dI}{4000}, \quad d\beta = \alpha \frac{dUI}{4000}, \quad \alpha \sim \frac{T_s}{0.02} \text{ A} \quad (10)$$

where:

$d\alpha U, d\alpha I$ – error of interval measurement between subsequent voltage samples u_1 and u_2 or current samples i_1 and i_2 ,

$d\beta$ – delay error of reading out the successive samples of voltage and current u_1, i_1 or u_2, i_2 ,

$A = 360$ degrees or $A = 2\pi$ radians,

T_s – sampling period.

The above errors have been determined by the measurement for various time periods (sampling periods) of $T_s = 25, 35, 45, 55, 65, 75, 85$ ms. The determined errors, in degrees, with respect to the sample numbers 1÷1000, are shown in Fig. 7.

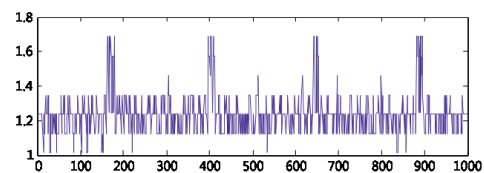
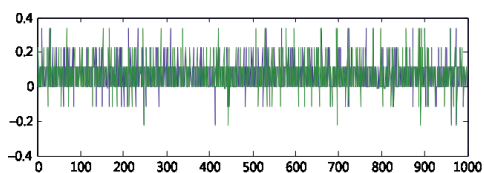


Fig. 7. $d\alpha U, d\alpha I, d\beta$ errors in degrees, for 50 Hz signals

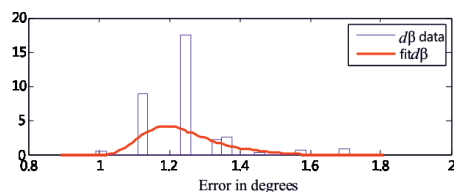
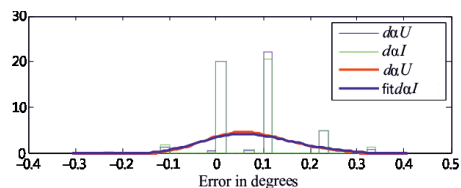


Fig. 8. Errors histogram for $d\alpha U, d\alpha I, d\beta$

Histogram example of errors $d\alpha U$, $d\alpha I$, $d\beta$ with fitted Generalized Extreme Value distribution are shown in Fig. 8.

Because the distribution of error probability is not a normal distribution, and it is also asymmetric, thus the error range for $d\alpha U$, $d\alpha I$, $d\beta$ has been defined as quantiles $p = 0.15$ and $p = 0.85$.

On the basis of the carried out measurements (Fig. 7) and analysis, the following errors of time measure and time delay have been assumed (see Fig. 9):

$$d\alpha I = d\alpha U = 0.11, d\beta = 0.4^\circ \div 1.2^\circ \tag{11}$$

what amounts respectively:

$$d\alpha I = d\alpha U = 6 \mu s, d\beta = 26 \div 80 \mu s \tag{12}$$

The relative error of active power P , formula (8), depending on the angle of the first acquired voltage sample u_1 (in time t_1) and for $\phi = \text{arctg}(k)$, where $k = Q/P$ is depicted in Fig. 10. This error has two components: the average $dP = d\beta \frac{\pi}{180} k$ (Fig. 11) and oscillating $d\dot{P}$ (Fig. 12).

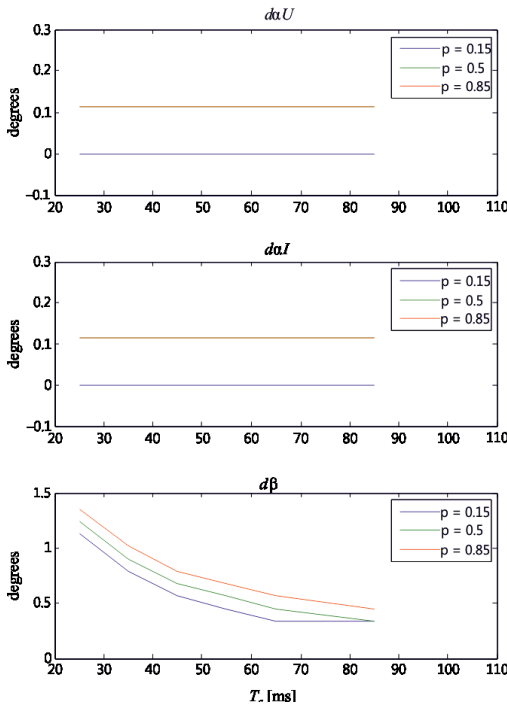


Fig. 9. Error of $d\alpha U$, $d\alpha I$, $d\beta$ dependence on sampling period T_s

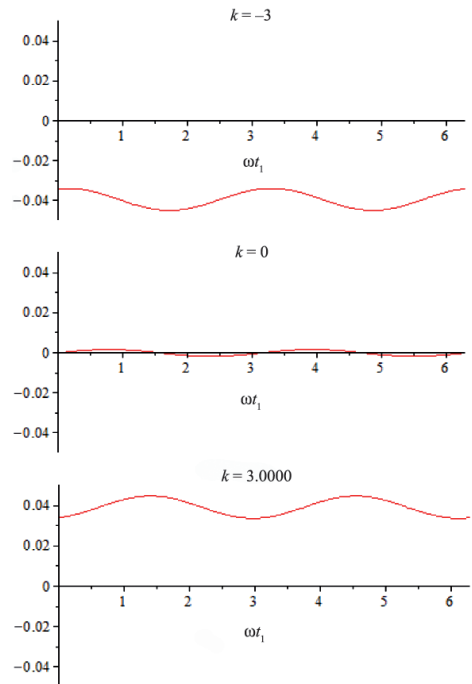


Fig. 10. The error of P dependence on the angle ωt_1 of the first acquired voltage sample

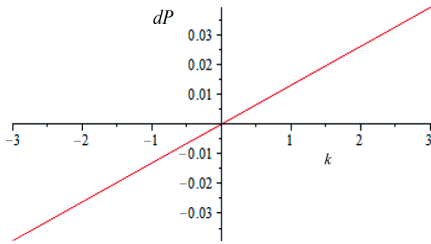


Fig. 11. The average relative dP error of active power P measurement

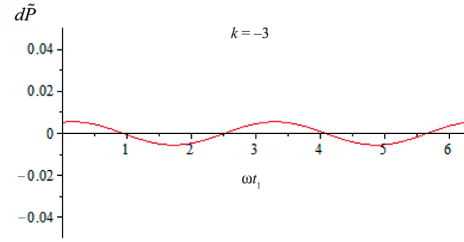


Fig. 12. Relative oscillating $d\tilde{P}$ error of active power P measurement

As can be seen from Fig. 11, the average relative error dP is proportional to k . The relative oscillating error $d\tilde{P}$ averages to zero after two consecutive samples distanced by $2\pi + \pi/2$.

The relative error of reactive power measurement $dQ = d\alpha \frac{\pi}{180} \frac{1}{k}$ according to (11), for $\phi = \arctg(k)$, where $k = Q/P$, is presented in Fig. 13.

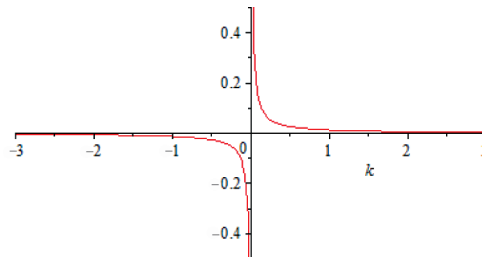


Fig. 13. The relative error of reactive power measurement dQ

As we can see, for $Q > P$, the relative error dQ is getting smaller, and for $Q \approx 0$, this error becomes big, but then the value of reactive power Q is close to 0. In order to check the performance of the microcontroller with different loads, samples readout and calculation of active P and reactive Q power for the different sampling periods (intervals) $T_s = 25, 35, 45, 55, 65, 75, 85$ ms and various $k = Q/P$ was carried out. The determined errors of measurements correspond to the theoretically predicted errors, which is shown in Fig. 14 and Fig. 15. For the reactive power $Q = 0$ only the absolute error is calculated, i.e. $dQ = Q - Q_0$. The analytically determined absolute errors $P_0 dP$ and $Q_0 dQ$ have their own statistical errors ddP and ddQ , which can be assumed constant – $ddP = 0.005$ and $ddQ = 0.002$.

It can be stated that the compensation of measurement error of active P and reactive Q power can be carried out in two ways:

- by taking into account the above errors; at first, the ratio $k = Q/P$ must be calculated, then actual values can be computed by the following formulas:
 - for active power: $P_0 = P \cdot (1 - dP(k) \pm ddP)$,
 - for reactive power: $Q_0 = Q \cdot (1 - dQ(k) \pm ddQ)$, for $k \approx 0$ the measured value of reactive power Q is not correct,

- or by taking into account the series sampling into the formulas for active P and reactive Q power (1), which will be the subject of further works concerning the implementation of low-frequency measuring methods for a two-terminal network.

For example, P and Q of a real RLC two-terminal network have been measured with the use of a PLC FX3G type with expansion board AD-BD, for which: $d\alpha I = d\alpha U = 0,11^\circ$, and $d\beta = 1.2^\circ$ (for $T_s = 25$ ms). The parallel measurement with the use of PLC with expansion board AD-BD has been carried out for comparison:

- the values measured by PLC are: $P = 320$ W, $Q = 924$ Var – Fig. 16,
- the values measured by laboratory meter are: $P_0 = 300$ W, $Q_0 = 920$ Var.

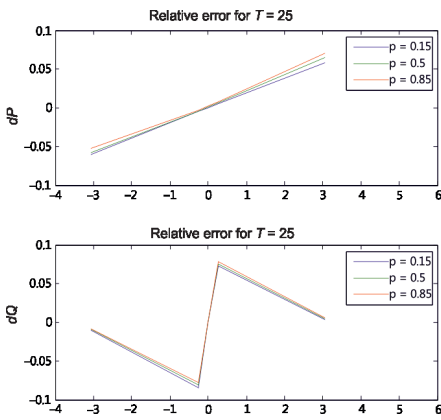


Fig. 14a. dP and dQ errors dependence on k for $T_s = 25$ ms

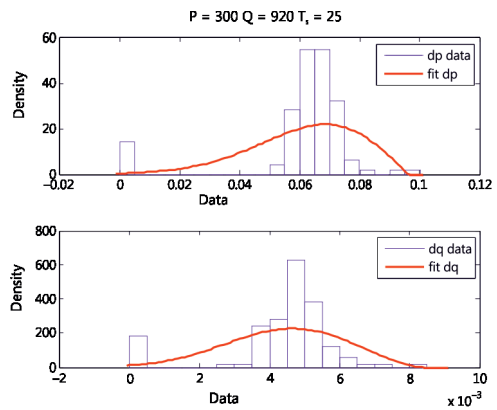


Fig. 14b. dP and dQ errors histogram for $P = 300$ W, $Q = 920$ VAR, $T_s = 25$ ms

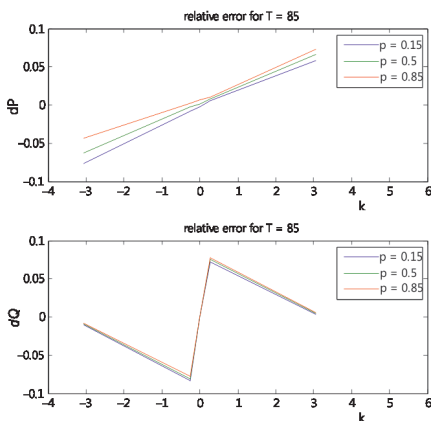


Fig. 15a. dP and dQ errors dependence on k for $T_s = 85$ ms

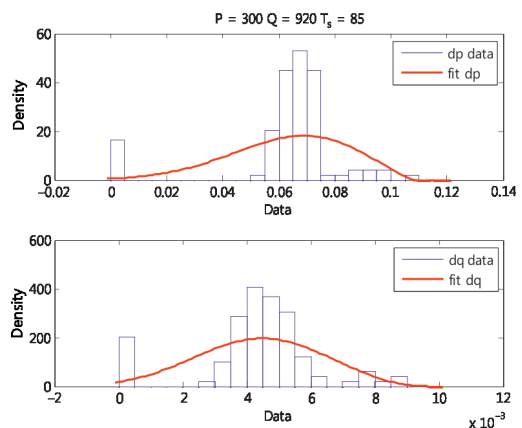


Fig. 15b. dP and dQ errors histogram for $P = 300$ W, $Q = 920$ VAR, $T_s = 85$ ms

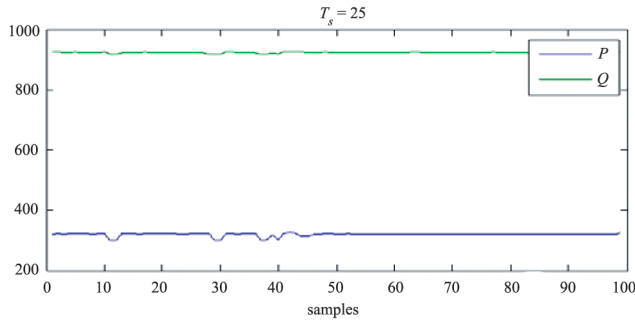


Fig. 16. An example of controller measurement results for $P = 300$ W, $Q = 920$ VAR and $T_s = 25$ ms

In order to correct the PLC measurement values of power, the k ratio is firstly calculated:

$$k = Q/P = 2.88, \quad (12)$$

then the systematic errors:

$$dP = d\beta \frac{\pi}{180} k = 0.06 \text{ and } dQ = d\alpha \frac{\pi}{180} \frac{1}{k} = 0.00066 \quad (13)$$

Thus the corrected values are:

$$P_0 \approx P \cdot (1 - dP(k) \pm ddP) = 300 \pm 1.5 \text{ W}, Q_0 \approx Q \cdot (1 - dQ(k) \pm ddQ) = 923 \pm 3 \text{ VAR} \quad (14)$$

and are almost identical to those measured by a laboratory meter.

It should be noticed that, although the RMS values of voltage and current are calculated as a square root of the formula for P , there is no delay error between the voltage – current samples $d\beta = 0$ and the oscillating error also averages to 0.

6. Conclusion

The article presents the low-frequency measuring method of current and voltage RMS values as well as the active P and reactive Q power of a two-terminal network supplied with a sinusoidal voltage of 50 Hz. This method has been implemented on a small, compact Mitsubishi FX3G type controller, having a relatively small computing power. Simultaneously, it has been running a typical control task on the controller. The measurement tests have been performed in a laboratory. On this basis, the impact of sampling period instability and delays in sampling on the results, caused by the real A/D converter board 2AD-BD, was verified.

Acknowledgment

The presented results of the research, which was carried out under the theme No. E-1/524/2016/DS, E-2/581/2016/DS, were funded by the subsidies on science granted by Polish Ministry of Science and Higher Education

References

- [1] Chwaleba A., Poniński M., Siedlecki A., *Electrical Metrology*, WNT, Warszawa 2003.
- [2] Jaraczewski M., Mielnik R., *The method of measuring the power of a two-terminal circuit and it's RMS voltage and current, when powered by sinusoidal alternating 50 Hz voltage (parallel sampling method)*, Patent Application P.415108.
- [3] Jaraczewski M., Mielnik R., *The method of measuring the power of the two-terminal circuit and it's RMS voltage and current, when powered by sinusoidal alternating 50 Hz voltage (series sampling method)*, Patent Application P.415109.
- [4] Jaraczewski M., Mielnik R., Sułowicz M., *The Low-frequency measuring method and signal processing application in electrical machines and electric devices monitoring*, Materiały XIII Konferencja Wybrane Zagadnienia Elektrotechniki i Elektroniki, WZEE'2016, Rzeszów 2016.
- [5] Jaraczewski M., Mielnik R., Sułowicz M., *The low-frequency measuring method and signal processing application in cage induction motors monitoring*, Maszyny Elektryczne – Zeszyty Problemowe Nr 2/2016 (110).
- [6] Krzyk P., *Wyznaczanie parametrów dwójnika zasilanego prądem sinusoidalnie zmiennym z użyciem algorytmu o minimalnej złożoności obliczeniowej*, Pomiar Automatyka Kontrola, 2012.
- [7] Ludwinek K., Chrzan K., *Konfiguracja modułów A/D i D/A sterowników PLC do pomiarów i sterowania. Napędy i sterowanie*, Nr 9, 2009, 46–52.
- [8] Ludwinek K., Chrzan K., *Programowanie modułów A/D i D/A sterowników PLC do pomiarów i sterowania. Napędy i sterowanie*, Nr 10, 2009, 70–75.
- [9] Jian Sun, Peng Lu, Yawing Fu, Ruixiang Liu; Le Chen, *The implementation and application of programming port communication between industry PC and Mitsubishi FX series PLC*, Proceedings of 3rd International Conference on Intelligent System and Knowledge Engineering, 2008.
- [10] FX3G Series Programmable Controllers User's Manual – Hardware Edition. Mitsubishi Electric 11/2015.
- [11] FX3S/FX3G/FX3GC/FX3U/FX3UC Series Programmable Controllers User's Manual – Analog Control Edition, Manual n-r JY997D16701; revision: H. Mitsubishi Electric 03/2016.
- [12] FXCPU Structured Programming Manual – Application functions. Manual n-r: JY997D34801, revision K. Mitsubishi Electric 04/2015.
- [13] FXCPU Structured Programming Manual – Basic & Applied Instruction. Manual n-r: JY997D34701; revision M. Mitsubishi Electric 04/2015.
- [14] FX Series Programmable Controllers User's Manual – Data Communication Edition. Manual n-r: JY997D16901, revision: F. Mitsubishi Electric 11/2009.3